Ground-state properties of finite square and triangular Ising lattices with mixed exchange interactions

E. E. Vogel, J. Cartes, S. Contreras, and W. Lebrecht
Departamento de Ciencias Físicas, Universidad de La Frontera, Casilla 54-D, Temuco, Chile

J. Villegas
Departamento de Física, Universidad de Concepción, Casilla 4009, Concepción, Chile
(Received 13 November 1992; revised manuscript received 23 September 1993)

Small Ising lattices with both ferromagnetic (F) and antiferromagnetic (AF) exchange interactions (or bonds) and increasing numbers of spins are studied by means of two independent methods: computational solutions to the Hamiltonian problem and topological counting of frustration paths. Equal magnitudes and concentrations are assumed for both types of bonds. Two different geometries are considered: square lattices (SL's) with coordination number 4 and triangular lattices (TL's) with coordination number 6. Two-dimensional samples with a total number of spins N between 4 and 64 are considered for SL's, while N is varied between 4 and 44 for TL's. They are distributed in two-dimensional arrays where periodic boundary conditions are imposed. After an array is selected, bond distributions (samples) are independently and randomly generated in fixed positions. The physical parameters are then calculated exactly for each sample. The emphasis here is on the ground-state properties and their dependence with size and shape for the two kinds of lattices. All magnitudes correspond to a basic statistics over a large number of samples for each array. The following magnitudes are reported: ground-state energy per bond, frustration segment, abundance of first excited states, remnant entropy, low-temperature specific heat, and site order parameters q, p, and h. Parameters p and h are introduced here, showing advantages over other similar magnitudes. The results are in good correspondence with analytic studies for the thermodynamic limit. This means that the spin site correlation (p) tends to vanish as N grows. However, we have found that the shape dependence modulates the behavior of these systems toward the thermodynamic limit. There is no tendency to vanish for the bond correlation parameter (h). For both kinds of lattices h might be a constant independent of size and shape.

I. INTRODUCTION

Spin lattices with mixed exchange interactions have been studied for about 15 years.[1] Originally proposed as a simple model to understand spin glasses, such lattices have found applications in several other fields.

In the present paper we want to go back to one of the original problems, which describes the ground-state properties of two-dimensional square lattices SL's (each spin surrounded by four equivalent neighbors) with mixed ferromagnetic and antiferromagnetic exchange interactions (or bonds as they will be referred from now on) of equal magnitude. Additionally we extend the application of the method described below to triangular lattices (TL's) (each spin is surrounded by six equivalent neighbors).

The present analysis is restricted to the case of an equal number of either type of bond. We perform exact calculations on samples increasing the number of spins N, varying the ways of distributing these spins in rectangular arrays, introducing the shape as one interesting feature. The lattices will be characterized by some usual parameters and two new ones to be defined below. The results of the numerical calculations will also be related to the topological properties of these systems.[2]

Most of the progress in this area has relied on approximate calculations by means of numerical treatments such as the Monte Carlo method,[3] analytical results valid for the thermodynamic limit,[4] and general topological treatments.[5] In this work we present the tendencies followed by small samples as they get progressively larger. We scan the relevant portion of the Hilbert space (or spin configurational space as it is usually called) looking for the low-energy states of each particular distribution of bonds, calculating the most representative parameters. In the next section we discuss the way this is done. The computer time involved in these exact calculations grows considerably. This is an important limitation for this kind of work and lead us to stop at $N=64$ for SL's, where we believe the main tendencies show clearly. In the case of TL's the convergence is more rapidly reached, so it is enough to reach $N=44$, to get a tendency similar to the one shown by SL's. This apparent difference is not such if we compare the number of energy contributions (the number of bonds) for the extreme cases: it is 128 for SL's and 132 for TL's. We will use here average values over 500 different bond distributions for the different parameters to be calculated below. This basic statistics gives results that are stable enough for this kind of array as we have proven recently.[6] All together we have solved the exact Ising Hamiltonian for about 100 000 different lattices.

The approach of this work is to present our results for

a large number of "computational experiments" on both well-known and new parameters used to characterize magnetic systems such as spin glasses. Two different techniques are used and will be described in next section.

In Sec. II, we briefly review the most relevant theoretical aspects introducing the basic definitions and notation. In Sec. III, we present the results in figures, where the independent variable is the number of spins N. The tendencies toward larger lattices (or toward the so-called thermodynamic limit) are discussed and compared with earlier results when applicable. Finally, in Sec. IV, some general and particular conclusions are obtained.

II. THEORY AND BASIC DEFINITIONS

Let us consider a two-dimensional lattice with L spins along one direction and M spins along the other direction. The total number of spins is then

$$N=L\times M \ . \tag{1}$$

We shall refer to N as the *size* of the lattice. For rectangular arrays we will follow the arbitrary notation that M will refer always to the side with fewer spins.

The spins lay on the vertices of such a lattice. A bond is defined along the straight line that joins two adjacent spins (nearest-neighbor interaction). A bond can be either ferromagnetic (F) or antiferromagnetic (AF) while the magnitude of the interaction J is the same in both cases and equal to 1 (one unit of energy). The total number of bonds will be denoted by B and it is $2N$ for SL's and $3N$ for TL's. We restrict ourselves here to the case of $B/2$ F bonds plus $B/2$ AF bonds. For TL's with an odd number of spins, lattices will have one more bond of a certain kind, which will be compensated as indicated below. The results reported below consistently make use of periodic boundary conditions.

We call each different combination of L and M for a given N an *array*. Thus, for 24 spins there are three different arrays: 12×2, 8×3, and 6×4. There are some sizes that allow just one kind of array as, for instance, $N=35$. For N less than 40 all the possible arrays are calculated in the case of SL's, while in TL's all cases under 30 were taken into account. Other considerations of the ways the different arrays were chosen can be seen from the figures containing the results. Generally speaking, arrays with M close to L were favored as the size increased. The scope of the numerical calculations is decided by the computer time limitations.

Within each array there are

$$D=\frac{(B)!}{(B/2)!(B/2)!} \tag{2}$$

different possible distributions of B bonds in the way presented above. Occasionally it is possible to subtract for equivalent samples considering translations, rotations, mirror images (reversing the signs of the bonds), or other symmetry properties. However, the number of possible different distributions grows essentially as the factorial function. Each possible fixed distribution of bonds will be called a *sample*. For a given array physical properties differ when going from one sample to another. In the analysis below we consider average values over many samples (500) to deal with results that can be compared with the natural self-averaging values that arise toward the thermodynamic limit.

As a way to gain some familiarity with the definitions, the reader is invited to look for the generalities in Figs. 1–3. In the first one we present a particular SL 4×4. Figure 2 represents another SL, this time for the array 3×2. In Fig. 3, we present a TL corresponding to a 6×4 array. A single bar represents a F interaction while a double bar stays for an AF bond. Other features contained in these figures will be discussed below.

Two different techniques will be used to get numerical results and perform the analysis: (i) a Hamiltonian approach, where numerical techniques are used to find the ground-state properties; and (ii) a topological approach, where some graphical techniques are used for the same purpose. We will now present the basic of these techniques defining along the way the main parameters that can be calculated by either approach.

A. Hamiltonian approach

The Hamiltonian can be written as

$$H=\sum_{i<j} J_{ij}S_iS_j \ , \tag{3}$$

where the sums extend over all of the different pairs of

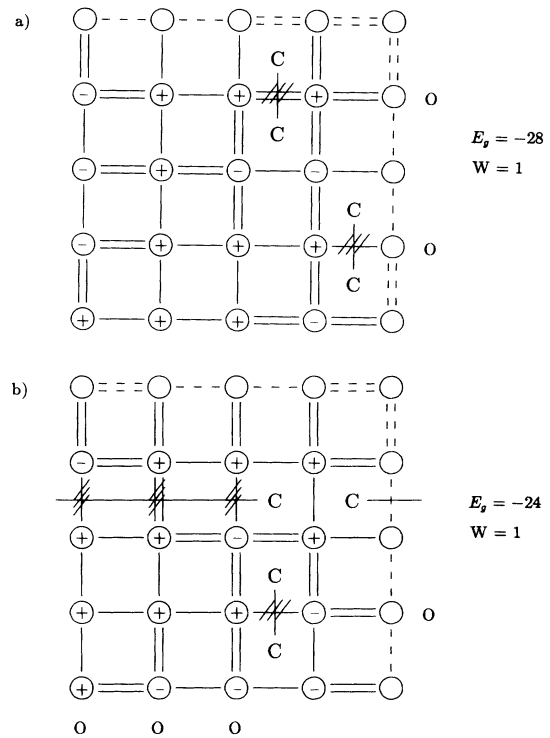

FIG. 1. Two different distributions of bonds for 4×4 lattices, showing the curved plaquettes marked by C and the odd bands marked by an O. Single and double bars represent ferromagnetic and antiferromagnetic bonds, respectively. Frustrated bonds are shown by dashed lines. Frustration segments are shown as straight lines. Signs represent the spins that define the ground state of the systems as found by the numerical calculation. Periodic boundary conditions are explicitly shown.

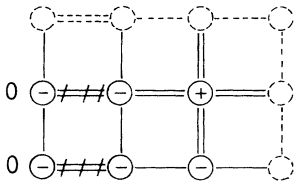

FIG. 2. An example of a 3×2 square lattice without any curved plaquette but with close loops of frustration segments due to the presence of odd bands. Signs correspond to one of the three possible ground states. The symbols were defined in Fig. 1.

nearest neighbors, S_i and S_j represent the third component of the spins at sites i and j, respectively. The bond between such a pair of spins is represented by J_{ij} and can be either -1 (ferromagnetic) or $+1$ (antiferromagnetic).

A *state* can be represented by the ordered collection of orientation quantum numbers, which can be either $+\frac{1}{2}$ or $-\frac{1}{2}$. A trivial change in the scales renders values $+1$ or -1, respectively, which is what will be used below. The Hamiltonian is diagonal in this representation. However, it is not obvious which states span the ground level of a particular sample. It appears that it will be necessary to go over the Hilbert space that possesses 2^N states. A small simplification occurs due to the invariance of the Hamiltonian with respect to inversion of all the spins, namely, $S_i \rightarrow -S_i$ for all i. It is then enough to deal with half the Hilbert space, namely, 2^{N-1} states.

We look here for the low-energy portion of the density of states and its related properties. Namely, we find E_g, the ground level energy, the degeneracy W of this level and the actual states to calculate several other parameters as described below.

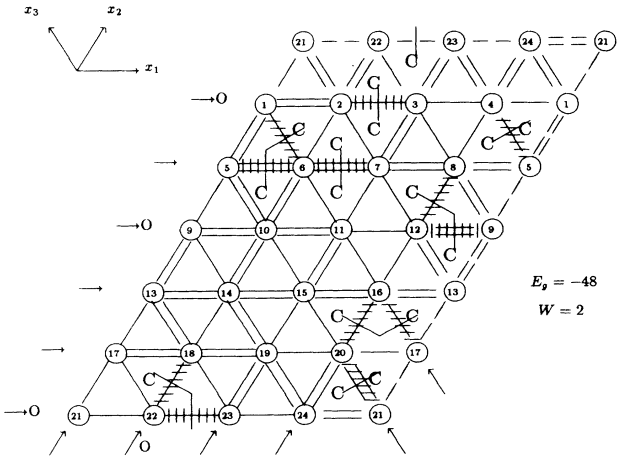

FIG. 3. An example of a 6×4 triangular lattice showing the curved plaquettes by means of a C and the odd bands by means of an O. Spins are numbered to allow for an easier identification of the two supernumerary bands. All independent bands are pointed out by arrows. One of the two degenerate ground states is shown by means of the frustration segments.

The algorithm begins with a quick approximate way of deciding the ground-state energy based on the replica method. This is achieved by randomly generating N^2 states, then for each state the method of steepest descent is applied to find the lowest possible energy. With this information an enumeration of the 2^{N-1} states is begun. However, the algorithm is constructed with logical decisions that avoid unnecessary calculations that would lead to energies larger than that of the supposed first excited level. If the partial enumeration finds an energy lower than the present one, the algorithm readjusts itself and continues from there on with the new ground-state energy. In this way the exponential computer times are dramatically reduced. The computer time turns out to be different for the different samples of the same type of array. It is small for the cases of lower energies and little degeneracy and large for the opposite cases.

Attention is also paid to the first excited level with energy E_g+4. The total degeneracy $U+V$ of this level has two components: the abundance U of secondary minima and the abundance V of states that belong to the same energy valley and are direct single-spin excitations from the ground state. In going from a ground state to a V state a single spin is flipped. On the other hand, in going from a ground state to a U state several spins must be flipped, eventually reaching saddle points with higher energy, before reaching the secondary minima.

To compare parameters for different sizes we look for intensive definitions of the relevant magnitudes. Thus, it is convenient to define the ground-state energy per bond:

$$\epsilon_g = \frac{E_g}{B} \ . \tag{4}$$

The remnant entropy σ is the most convenient way to look at the degeneracy W of the ground level. These two quantities are related by

$$\sigma = \frac{\ln W}{N} \ . \tag{5}$$

The magnetization per spin μ can be readily defined as

$$\mu = \frac{\sum_{\alpha}\sum_{i}^{N} S_i^{\alpha}}{NW} \ , \tag{6}$$

where S_i^{α} represents the value of spin at site i for one of the states α belonging to the microcanonical ensemble, namely, to the ground level. In this way μ takes values between -1 and $+1$.

Correlations C_ν to any order of neighbor ν can be defined in the following way:

$$C_\nu = \frac{\sum_{\alpha}\sum_{i}^{N}\sum_{j(\nu)} S_i^{\alpha} S_{j(\nu)}^{\alpha}}{n_\nu NW} \ , \tag{7}$$

where n_ν is the number of neighbors of order ν, while the sum over $j(\nu)$ includes all of them.

The site correlation can be investigated by means of the parameter q defined by Edwards and Anderson.[7] We calculate this parameter by means of the following expression:

$$q=2\frac{\sum_{\alpha\le\beta}\sum_{i}^{N}S_i^{\alpha}S_i^{\beta}}{NW(W+1)}\ , \tag{8}$$

where α and β play the role of initial and final states within the ground manifold. Each pair of states is counted once and the case $\alpha=\beta$ is allowed. In this way the total number of pairs is $W(W+1)/2$, which appears as a normalizing factor. The parameter q is then restricted to the interval $[-1,1]$.

If the entire Hilbert space is used for these calculations, all the off-diagonal contributions tend to compensate giving a result for q that trivially tends to zero as N grows. It is not obvious how to separate ergodic valleys in these systems. In lattices with net magnetism the initial application of a small magnetic field (which is taken to be zero after completing the calculations) is an effective way of performing the task. However, the density of states is a maximum at zero magnetization. What we have done is to look for one of those spins that are strongly bound, which means that its four surrounding bonds are not frustrated for one of the ground states. Then we pick an arbitrary sign for it. All the remaining ground states (if any) with this sign for the chosen spin are said to belong to the same half the Hilbert space. States with opposite sign for this spin are left out of consideration. We understand that this is an arbitrary way of deciding upon the ergodic valley in which the calculations will be performed. Different criteria on this matter might lead to slightly different results for those parameters that are strongly dependent on this decision.

All of the above parameters follow well-known definitions and have been applied to different magnetic systems. However, it does not seem that they are very adequate for lattices with mixed bonds. On the other hand, correlations to any order and magnetization, average to zero over a large number of samples, for any given N. That is to say, these parameters do not discriminate any behavior in these systems.

We introduce here a new site parameter p, which is more drastic than q and diminishes faster than q as N increases. Let us define p in the following way:

$$p=\frac{1}{N}\sum_{i}^{N}\left\{\left|\sum_{\alpha}S_i^{\alpha}\right|\mathrm{div}\,W\right\}\ , \tag{9}$$

where $|\ |$ means absolute value while div represents an integer division, so the result inside $\{\ \}$ can be either 0 or 1.

A simple way to compare p and q is the following. When going through the different states that form the ground level a certain spin can flip several times. Such a spin contributes to the calculation of q with a given weight, which is smaller for those spins that flip more. In the calculation of p a single spin flip means a zero value for such a weight factor. That is to say, p measures the fraction of the spin lattice that never changes when going through the ground level. From this discussion follows that

$$p\le|q|\ . \tag{10}$$

Anyhow, the calculations of p require deciding upon the ergodic valley corresponding to half the Hilbert space. This is done in the same way as it was already discussed for the case of q. (Considering the whole Hilbert space always gives $p=0$ as can be easily proven.)

It would be advantageous to have a magnitude that does not depend on the ergodic valleys of the Hilbert space. With this purpose we have defined a new parameter h, whose value is the same when considering half or the whole Hilbert space. We define the fraction of bonds that never frustrate h in the following way:

$$h=\frac{1}{B}\sum_{i<j}\left\{\sum_{\alpha}^{W}\frac{|S_i^{\alpha}S_j^{\alpha}-J_{ij}|}{2}\mathrm{div}\,W\right\}\ , \tag{11}$$

where the first sum extends over the B pairs of nearest neighbors (i,j) and we make use of the integer division introduced in Eq. (9). Theoretically the range for h would be [0,1], but we will see that the actual values fluctuate around 0.5.

B. Topological approach

The topological properties of these lattices provide an alternate way to find the ground states. The smallest closed circuit of bonds is called a plaquette.[8] The plaquettes that involve an odd number of AF bonds cannot satisfy the requirements of all its bonds; it is then said that such a plaquette if *frustrated* or *curved* (C). Otherwise the plaquette is normal or *flat*. The total number of curved plaquettes (always an even number) will be denoted by P_C. It has been proposed[2] that the energy of a particular state can be found by joining the curved plaquettes in pairs. This is achieved by means of *frustration segments* that go from the center of one curved plaquette to the center of another one, frustrating the bonds that are crossed by the frustration segment.

It follows that the total number of frustration segments is $P_C/2$. The *length of a segment* is the number of frustrated bonds that are associated to it. All of the frustration segments add up to the *frustration length* Λ_F. The ground level comprises those cases of minimum Λ_F, denoted by Λ_{Fg}, which corresponds to the least frustration in the system. The degeneracy of the ground level is the number of different ways in which a set of frustration segments can be drawn keeping Λ_{Fg} to its minimum possible value.[9]

We can define the *average frustration segment* $\langle\lambda_{Fg}\rangle$ for the ground level of a given sample as

$$\langle\lambda_{Fg}\rangle=\frac{2\Lambda_{Fg}}{P_C}\ , \tag{12}$$

where the symbol $\langle\ \rangle$ means average over a particular sample. The energy E_g corresponding to the ground state can then be expressed as

$$E_g=-B+2\Lambda_{Fg}\ . \tag{13}$$

The energy per bond is then simply written as

$$\epsilon_g=-1+\frac{2\Lambda_{Fg}}{B}\ , \tag{14}$$

or in the more meaningful expression:

$$\epsilon_g = -1 + \frac{P_C \langle \lambda_{Fg} \rangle}{B} , \tag{15}$$

where the balance between the number of curved plaquettes and the average frustration segment can be appreciated.

The aim of the topological method is to find both Λ_F and the number of different ways to get the same value for Λ_F. These parameters depend primarily on the distribution of curved plaquettes as follows from the proposal of Toulouse.[2] However, we also found that they also depend on the topological characteristics imposed by the boundary conditions. To realize this, let us define as *band* the minimal circuit that can be closed by means of the boundary conditions in each independent direction. There are then $L+M$ bands for SL's. A band will be said to be *even* when it possesses an even number of AF bonds and *odd* otherwise.

In Fig. 1, we reproduce two different 4×4 square samples that are equivalent as far as the distribution of the four curved plaquettes is concerned. However, it is found from the numerical calculation that they have distinct values for Λ_{Fg}. The topological and numerical calculations can be matched if we add the condition that the curved plaquettes must be joined in pairs preserving the parity of the bands. If we look at the parity of the bands in the two lattices of Fig. 1, we realize that these two samples are no longer equivalent.

Another illustration on the importance of the bands is shown in Fig. 2 for a 3×2 square lattice with no curved plaquettes at all. However, the parity of the bands decides a basic frustration for this lattice that is readily found by the numerical calculations.

In the case of triangular lattices the same topological definitions apply. A particular example is presented in Fig. 3. The plaquettes are now triangular and there are three different directions on which bands can be defined. However, it turns out that two of these directions can be picked freely while the number of independent bands along the third direction depends strongly on the geometry of the array. We call these bands *supernumerary* since they are not present in SL's and since the number of them fluctuates between 1 and M. It has been proven[10] that the number of supernumerary bands η is given by

$$\eta = \max(l \cap m) , \tag{16}$$

where l represents the set of all the divisors of L and m represents the set of all the divisors of M. Namely, η is the maximum common divisor of both L and M.

This can be applied to Fig. 3 where we represent a 6×4 TL. There are then two supernumerary bands. This can be verified by closing the lattice using periodic boundary conditions. There are six bands parallel to the x_1 axis, there are four bands along the direction of the x_2 axis, while the bands along the direction of axis x_3 interconnect themselves forming two independent helicoidal bands.

We will not get deeper into the topological discussion since we use topology here as a mere technique to calculate the properties of spin lattices. Nevertheless, there is abundant literature that relates the physical parameters of the Ising lattices to their corresponding topological properties.[11,12]

III. RESULTS AND DISCUSSION

Given a particular size (N) and shape (L,M), 500 samples were prepared for both SL's and TL's generating randomly the locations for $B/2$ ferromagnetic and $B/2$ antiferromagnetic bonds. The bonds are frozen in their original positions. A computer code was prepared to scan the lower-energy portion of the Hilbert space. For small enough samples ($N \leq 30$) a great amount of information was extracted. However, as the size grows the computer time increases enormously. For larger samples we concentrated mainly on the relevant properties of the ground state which is what we report below in terms of average values over the 500 samples corresponding to each array.

In the case of TL's with odd N it happens that $B/2$ is not an integer number. Then 250 samples are generated with $(B+1)/2$ F bonds and $(B-1)/2$ AF bonds, while the remaining 250 samples correspond to the permutation of these assignments. However, we must point out that no appreciable differences appear and we have done this refinement with the only idea of strictly preserving equal concentration of both kinds of bonds through all of the arrays.

Both periodic and antiperiodic boundary conditions were used. For a given sample dramatic changes may occur when switching to different boundary conditions. However, after the statistical treatment the differences tend to disappear. In the present paper we use periodic boundary conditions only.

Using the techniques outlined in the previous section several physical and topological quantities were calculated for each sample. In Figs. 4–11, we give the results for the main parameters superimposing the results for TL's and SL's. The ordinate is the size N while the vertical axis is broken to allow for both types of lattices.

The ground-state energy per bond as a function of size is shown in Fig. 4. Different symbols denote the different shapes according to the shorter side of the array (M): Thus, for lattices $?\times2$ plus signs are used, while in $?\times3$ lattices, triangles are used. Other cases are explained in the figure themselves. Small lattices show a larger energy per bond, which decreases quickly to an asymptotic behavior of about -0.70 for SL's. This is consistent with numerical estimations for the thermodynamic limit.[4] In the case of TL's, ϵ_g tends asymptotically to a value that can be estimated at -0.56. A lower bound value can be obtained by the ideal case in which the number of curved plaquettes is precisely half the number of plaquettes (maximum of the distribution) and the frustration segment is 1.0, the minimum possible value when all pairs of curved plaquettes share a frustrated bond. Then the values of -0.75 and -0.67 are obtained for ϵ_g in the cases of SL's and TL's, respectively, as also shown in Fig. 4.

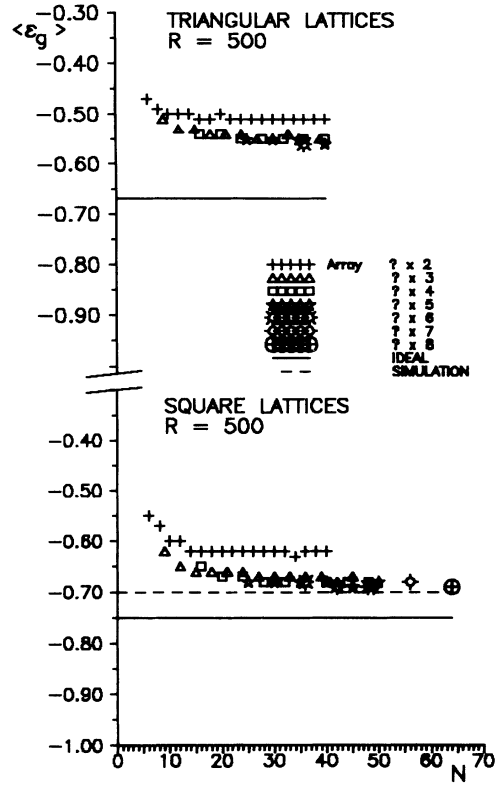

FIG. 4. Ground-state energy per bond ϵ_g as a function of size N. The shape is represented by the side with fewer spins. The solid line represents the ideal lower bound discussed in the text, while the dashed line represents the asymptotic behavior of large lattices as obtained from approximate calculations.

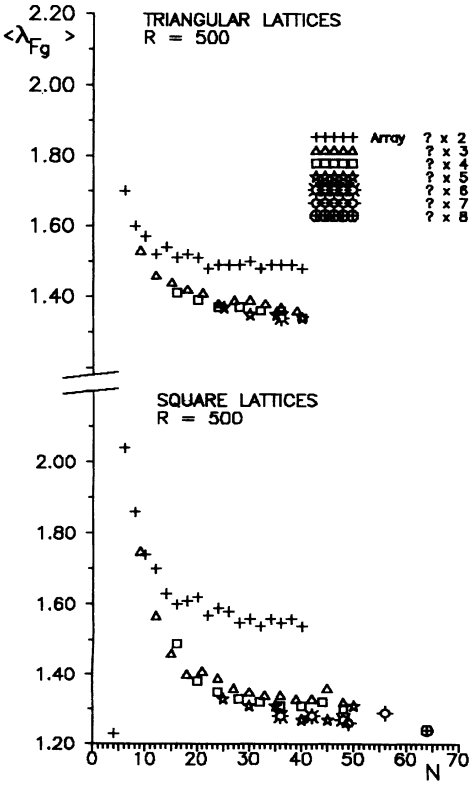

FIG. 5. Average frustration segment $\langle \lambda_{Fg} \rangle$ for the ground manifold as function of size and shape.

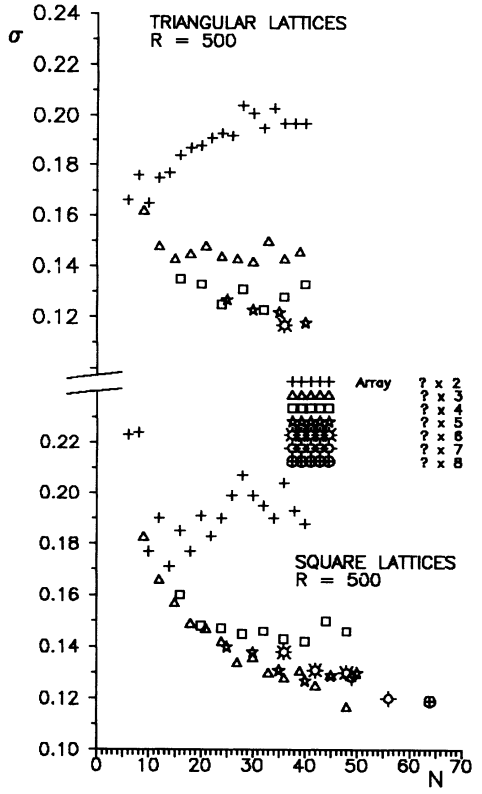

FIG. 6. Remnant entropy σ as function of size and shape.

Lattices with $M=2$ present a clear shape dependence. They tend to saturate at about -0.63 for SL's and at -0.50 for TL's. Since there is no similar indication for any other shape, we conclude that this is a peculiar behavior of these extremely narrow lattices, which are not truly two dimensional in the sense that a spin interacts with the same neighbor in opposite directions. Due to this peculiarity we stopped the calculations for ar-

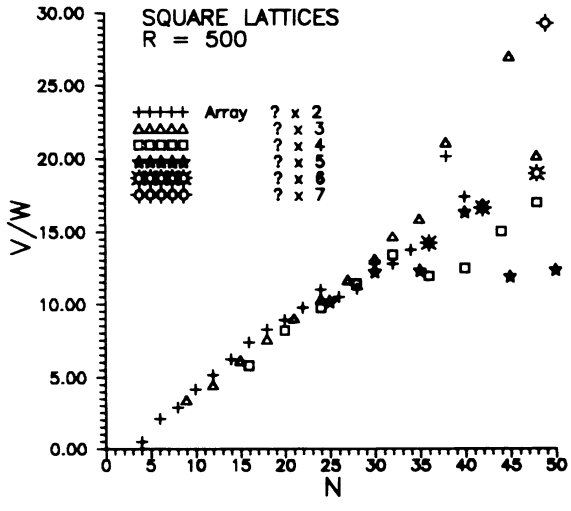

FIG. 7. Relative degeneracy of states that are direct excitations from the ground states, as function of size and shape (square lattices only).

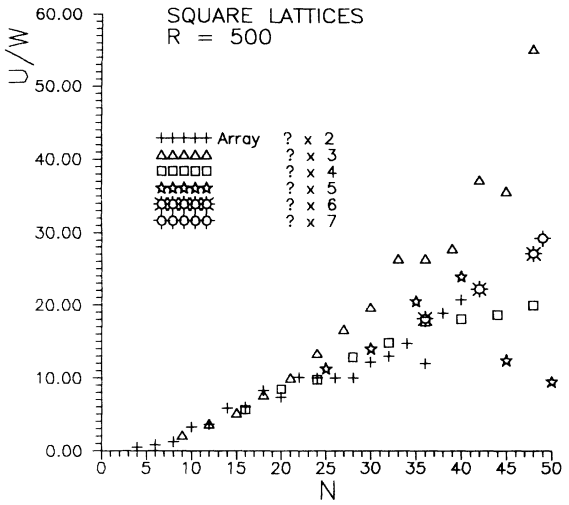

FIG. 8. Relative degeneracy of states that are secondary minima with energy E_g+4 and cannot be obtained as single excitations from ground states, as function of size and shape (square lattices only).

rays with $M=2$ earlier than for the rest of the arrays. Other than this peculiar feature of both square and triangular arrays with $M=2$, there is no other shape dependence for the energy of the ground manifold.

By means of Eq. (15), and knowing the number of curved plaquettes for each sample, we can study the behavior of the average frustration segment $\langle \lambda_{Fg} \rangle$. Then the statistics over the 500 samples is performed and these results are presented in Fig. 5. For the case of SL's we notice that $\langle \lambda_{Fg} \rangle$ can be as high as 2.0 for $N=6$, decreasing toward a value close to 1.2 in the thermodynamic limit. Interesting enough, if we feed this numerical value back into Eq. (15), for the most common system with $N/2$ curved plaquettes, we obtain $\epsilon_g=-0.70$. The main tendency of saturation is also shown by TL's where the same exercise can also be done. In these systems the distribution maximizes at N curved plaquettes, yielding $\epsilon_g=-0.56$ as the asymptotic value in Fig. 4.

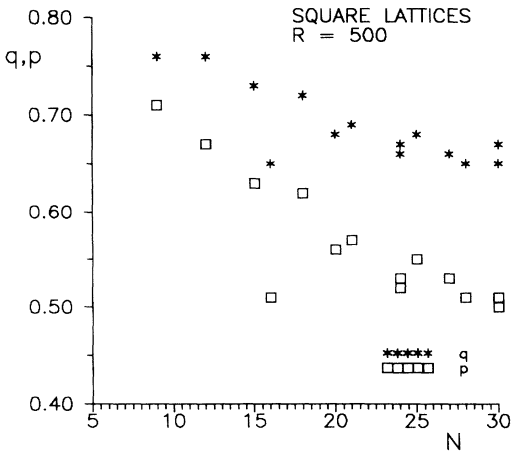

FIG. 9. Comparison of spin site correlation parameters q and p as functions of size up to $N=30$, for square lattices.

The shape dependence of $\langle \lambda_{Fg} \rangle$ is also presented in Fig. 5 and it is found to be very similar for the two systems under consideration. As can be seen in Fig. 5, $\langle \lambda_{Fg} \rangle$ decreases when the array approaches the square shape. Anyhow, the case $M=2$ departs from the main stream for both systems. The previous discussion for ϵ_g also applies here.

The degeneracy W of the ground level (half the Hilbert space) is better studied by means of the remnant entropy σ as expressed in Eq. (5). This is presented in Fig. 6 as a function of size and shape using the same symbols defined in previous figure. The size dependence for SL's tends to saturate at a value close to 0.11. This value is larger than 0.07 obtained in early applications of the method of Toulouse,[9] where the parity of the bands was not considered. For TL's the saturation value is also close to 0.11.

Perhaps the most interesting point in discussing σ is its shape dependence which shows quite different behavior in the two kinds of lattices under consideration. For both systems the saturation value tends to be a property of M the number of spins in the shorter side. However, while in TL's this value decreases with increasing M, in SL's the saturation values show alternate behavior: odd sides of M showing lower remnant entropy. Then as M grows the thermodynamic limit is to be found as the lower envelope of the TL points, while it shows an intermediate behavior for SL's. This is clearly a topological property that we point out here as a result without attempting a demonstration which is beyond the scope of this work.

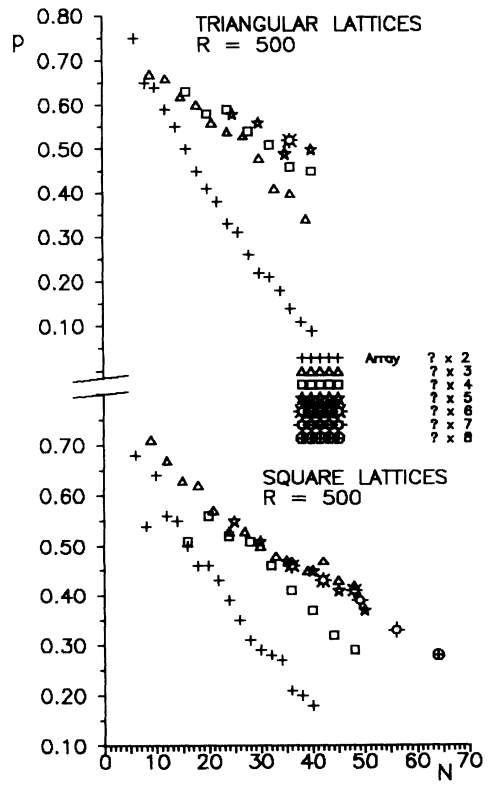

FIG. 10. Spin site correlation parameter p as function of size and shape.

Another important size effect related to the degeneracy of the ground state is that the presence of ground singlets tends to disappear rather quickly as N increases.[6] This means that there is a diminishing probability that the ground-state properties of these systems are uniquely defined.

Let us now depart momentarily from the main line that deals with the ground level. For thermal processes the excitations within a certain energy valley, or direct excitations from the ground state, are the most important ones. This is particularly true for low temperatures. Although we are mainly interested here in zero-temperature properties, let us make use of Fig. 7 that allows to study the low-temperature behavior of the specific heat for SL's (the analysis can be easily extended to TL's). At zero temperature the system is trapped in a particular ground state that we can visualize at the bottom of a certain energy valley. As temperature rises only direct excitations or single spin-flip excitations of minimal energy ($4|J|$) will take place. Then, in the low-temperature limit (T measured in units of $|J|$), the local partition function around one of the ground states is given by

$$Z(T)=W+Ve^{-4/T}, \tag{17}$$

that leads to an asymptotic specific heat of the form

$$C(T)=\frac{16}{T^2}\frac{V}{W}\frac{e^{4/T}}{[V/W+e^{4/T}]^2}. \tag{18}$$

We realize that the specific heat is governed mainly by the ratio V/W (the ratio between the degeneracy of the first direct excitations and the degeneracy of the ground state).

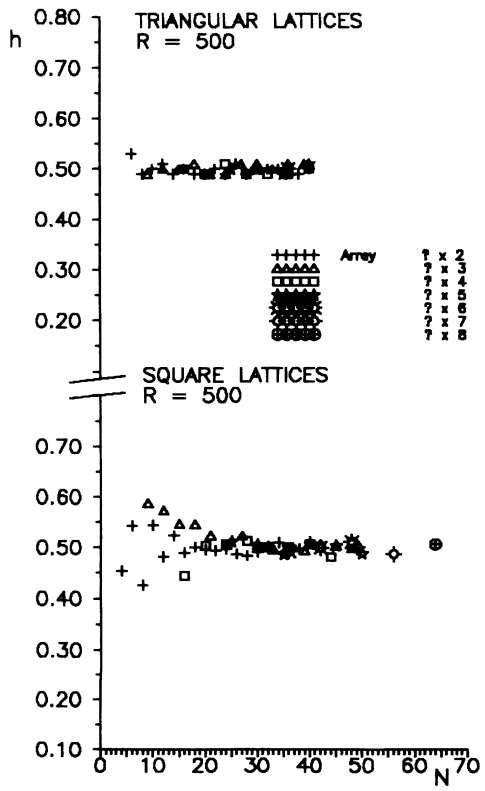

FIG. 11. Bond site correlation parameter h as function of size and shape.

Even for a given energy valley the degeneracy of the ground level could be large due to the several spins that can be at zero-field positions (surrounded by the same number of satisfied and frustrated bonds). So we look for a representative valley looking for the average value of V/W for a given sample and then taking the statistical average over the 500 samples. As Fig. 7 shows this is essentially a linear function of N, which makes the "molar" specific heat $C(T)/N$ a true intensive variable of the system. The low-temperature specific heat does not show important corrections due to size or shape for small lattices. The scattering of the data increases rapidly with N. We believe that such instability is associated with the lack of precision of V within 500 samples only.

We can also count the number of energy valleys U, each having a minimum energy exactly given by E_g+4, which we call secondary minima. In Fig. 8, we report the ratio of the number of secondary minima U over the degeneracy of the ground level W. Evidently U/W increases faster than linearly as a function of N. This is quite important because each local minimum is a potential attractor for this kind of systems. Thus, for instance, a very low temperatures a Monte Carlo calculation could be trapped by any such minimum without the possibility of reaching a true ground state in finite computational times. On the other hand, the onset of shape dependence is also showing in the behavior of arrays with $M=3$ that possess the largest relative number of secondary minima. We present results up to $N=40$ only, due to the instabilities showed by the statistical averages for larger lattices.

Let us go back to the ground-state properties of these systems. Although not graphically reported here we calculated magnetization and correlations to first- and second-nearest neighbors for all of the samples in all different sizes and shapes. As it can be expected, their average value is zero, with a standard deviation that decreases with size. The site correlation or q order parameter introduced by Edwards and Anderson,[7] defined in Eq. (8), was calculated for all samples up to $N=30$ in SL's. Then, a new parameter p was defined as given by Eq. (9), which shows faster convergence toward the thermodynamic limit. This is shown in Fig. 9, where both q and p are compared for the case of SL's. We can recognize that the theoretical relationship given by Eq. (10) is clearly satisfied. Moreover, there is a complete resemblance between the functional dependencies of p and q with respect to N. An important advantage of the new parameter is that the computer time needed to calculate p is much smaller than the one used to compute q. From now on we restrict our discussion to the p parameter defined in the present paper.

The dependencies of p on both size and shape are presented in Fig. 10. It can be seen that p goes to 0 as N goes to infinity for both SL's and TL's. The general slope is about the same for both systems. However, there are some clear differences with respect to the shape dependence in a way similar to what already was discussed before. Namely, TL's show a monotonic increase with the slope as M increases, while SL's show an alternate

behavior in which the samples with an even number of spins in the shorter side show a more pronounced decrease for p. Before abandoning this discussion we should remember that both p and q are dependent on the choice of the ergodic condition as discussed above.

We have defined a parameter h in Eq. (11), which does not depend on the choice of an ergodic condition. This parameter searches for those bonds that never frustrate as we run over all the states degenerate in the ground level. The fraction between this number and the total number of bonds gives h. The physical interpretation is that h represents the fraction of the lattice bonds that remain without frustration as we scan the states of the ground manifold. A concept related to this, called rigidity, had already been introduced.[5] However, in the case of rigidity the search was for bonds that either always frustrate, or just the opposite they never frustrate. Another way of realizing rigidity would be that of a bond that keeps its two spins in the same relative orientations in all ground states.[5] In spite of some resemblance to this rigidity, h is an entirely new quantity. An additional positive element is that the numerical evaluation of h does not require long computer times.

The dependence of h on N is presented in Fig. 11, for both kinds of lattices. There is one common feature: the general tendency is to oscillate around 0.5 in both cases, *without a particular size or shape dependence.* This independence is so clear that even the lattices with $M=2$ do not show any deviation as in all the previous properties. There is no dependence on the even or odd value of M either. The result tends to indicate that h is not dependent on geometry, topology, shape, or size as N goes to the thermodynamic limit. The behavior of h with respect to size and shape is not similar to any of the previous magnitudes.

Coming back to Fig. 11, it can be noticed that there are pronounced fluctuations for h in SL's, particularly for sizes under 30 spins, which are not shown by TL's. At first look, it looks like scattered data. Due to this fact we performed two different tests on the stability of the data shown in this figure. On the one hand, we repeated the *experiment* on two additional sets of 500 samples under 30 spins: the result is that the figure stays basically the same without a pronounced change in any of the points. On the other hand, we performed a progressive statistics for the square arrays up to 1000 samples: the result is that the average value of h reported in Fig. 11 is quite stable even for over just 60 samples.

The second of these observations deserves a deeper discussion. In Fig. 12, we present the progressive analysis for 1000 samples corresponding to 6×6 arrays. The statistics is updated every 20 samples. If we designate by r the sequential number of a particular sample or run, we perform independent statistics for $r=20$, 40, 60, 80, etc. The average values thus found are represented by the solid circles in Fig. 12. On top of that we also give the statistical deviations from this value in the form of error bars. Three comments are in order. First, $\langle h \rangle$ is close to 0.5 with very slight deviations for $r \geq 60$. Second, the standard deviations slowly decrease for small values of r, tending to a stable value. Third, similar behavior is

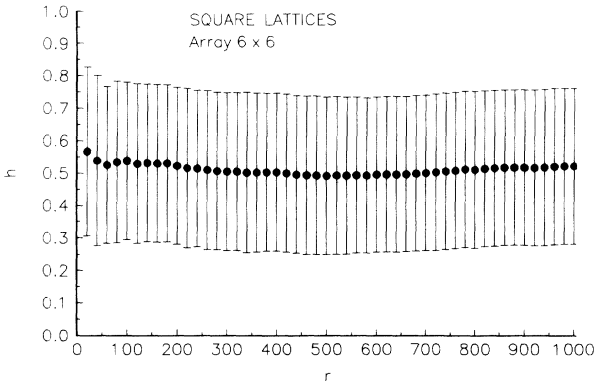

FIG. 12. Progressive statistical analysis of h as a function of the number of runs r included in the statistics, for square arrays 6×6. The standard deviations are illustrated as error bars.

shown by the other square lattices for which the same analysis was performed. However as the size increases the distribution of h sharpens and the error bars decrease slowly.[13] The fact that $h=0.5$ in both SL's and TL's could lead us to think that half of the bonds never frustrate for this kind of lattices, no matter as large these systems grow.

IV. CONCLUDING REMARKS

Small Ising lattices with mixed exchange interactions present frustration that modulates the properties of the system by size and shape. The topological properties are better understood if the frustration along the boundary conditions is shown explicitly by means of the parity of the bands. When this is done, total agreement is obtained between Hamiltonian and topological techniques applied to each particular problem.

Specific heat does not show evidence for dependence on either size or shape of square lattices. The general behavior of the "molar" specific heat is that of an intensive variable.

Ground-state energy of both SL's and TL's shows a dependence with size for small samples ($N \leq 30$) that very quickly disappears for larger values of N. The asymptotic limit for very large values of N is about -0.70 for SL's and -0.56 for TL's. No shape dependence is observed.

The remnant entropy σ of the system, also tends toward a saturation value of about 0.11 for both SL's and TL's. There is a strong modulation of the shape on this property that is more pronounced as the system departs from the square shape. A successful way of segregating this behavior is to characterize the samples by the side with less spins (M). It is then found that for SL's, σ tends to alternate saturation values as M increases in steps of one unity. However, the behavior for TL's is that the saturation values decrease monotonously as M grows.

The average frustration segment $\langle \lambda_{Fg} \rangle$ approaches its saturation value from above as N increases. In SL's and in TL's the shape dependence is characterized by M in a monotonic way: the larger M is, the lower is the asymptotic value.

The two new order parameters defined here present a behavior that shows that they represent a property of the lattices. The parameter p varies much faster than the Edwards-Anderson parameter q and is less time consuming for computer calculation. On the other hand, the parameter h shows a clear tendency to be a constant independent of size and shape.

In the case of p, the thermodynamic limit is reached much quicker for shapes with even and small values of M in the case of SL's. On the other hand, in the case of TL's there is a direct general correspondence: p decreases more strongly with size for smaller values of M in a monotonic way.

The parameter h was defined in order to avoid ergodicity problems. On top of that we encountered that for both SL's and TL's h tends to a constant value of about 0.5 as N grows, without a shape dependence. A sort of erratic but reproducible dependence on size is observed for very small samples (under 30 spins for SL's and under 10 spins for TL's).

Except for the case of h in all the other parameters the results for samples with $M=2$ (only two columns or rows) depart clearly from the rest. This is due to the fact that these arrays are not truly two dimensional since each spin is surrounded by the same neighbor along two different directions. Due to the higher coordination number for TL's, as compared to SL's, these samples showed a more rapid convergence to the saturation value of each result.

ACKNOWLEDGMENTS

This work has been partially funded by FONDECYT (Chile) under Contract No. 1930385, Dirección de Investigación y Desarrollo (Universidad de La Frontera), and Dirección de Investigación (Universidad de Concepción). One author (E.E.V.) is also grateful to the Fulbright Foundation for financial support that allowed to enjoy the hospitality of The Johns Hopkins University, where part of this work was performed.

[1]K. Binder and A. P. Young, Rev. Mod. Phys. **58**, 801 (1986).
[2]G. Toulouse, Commun. Phys. **2**, 115 (1977).
[3]K. Binder and D. Stauffer, in *Applications of the Monte Carlo Method in Statistical Physics*, edited by K. Binder (Springer-Verlag, Berlin, 1984).
[4]M. Mezard, G. Parisi, and M. A. Virasoro, *Spin Glass Theory and Beyond* (World Scientific, Singapore, 1987).
[5]F. Barahona, R. Maynard, R. Rammal, and J. P. Uhry, J. Phys. A **15**, 673 (1982).
[6]E. E. Vogel, S. Contreras, J. Cartes, and J. Villegas, in *Physics and Chemistry of Finite Systems: From Clusters to Crystals*, edited by P. Jena, S. N. Khana, and B. K. Rao (Kluwer Academic, Amsterdam, 1992), p. 813.
[7]S. F. Edwards and P. W. Anderson, J. Phys. F **5**, 965 (1975).
[8]I. Ono, J. Phys. Soc. Jpn. **41**, 345 (1976).
[9]J. Vannimenus and G. Toulouse, J. Phys. C **10**, 537 (1977).
[10]W. Lebrecht, Dissertation for Magister Degree, Universidad Austral de Chile, 1992.
[11]I. Bieche, R. Maynard, R. Rammal, and J. P. Uhry, J. Phys. A **13**, 2553 (1980).
[12]R. Maynard and R. Rammal, J. Phys. Lett. **43**, L347 (1982).
[13]E. E. Vogel, S. Contreras, and J. Cartes (unpublished).